University of Illinois at Urbana-Champaign

ACRC

Air Conditioning and Refrigeration Center A National Science Foundation/University Cooperative Research Center

Refrigerant-Side Tradeoffs in Microchannel Evaporators

T. Kulkarni, C. W. Bullard, and K. Cho

ACRC TR-198 June 2002

For additional information:

Air Conditioning and Refrigeration Center
University of Illinois
Mechanical & Industrial Engineering Dept.
1206 West Green Street
Urbana, IL 61801

(217) 333-3115

Prepared as part of ACRC Project #124
Design Tradeoffs in Microchannel Heat Exchangers
C. W. Bullard, Principal Investigator

The Air Conditioning and Refrigeration Center was founded in 1988 with a grant from the estate of Richard W. Kritzer, the founder of Peerless of America Inc. A State of Illinois Technology Challenge Grant helped build the laboratory facilities. The ACRC receives continuing support from the Richard W. Kritzer Endowment and the National Science Foundation. The following organizations have also become sponsors of the Center.

Alcan Aluminum Corporation
Amana Refrigeration, Inc.
Arçelik A. S.
Brazeway, Inc.
Carrier Corporation
Copeland Corporation
Dacor
Daikin Industries, Ltd.
Delphi Harrison Thermal Systems
General Motors Corporation
Hill PHOENIX
Honeywell, Inc.
Hydro Aluminum Adrian, Inc.
Ingersoll-Rand Company
Kelon Electrical Holdings Co., Ltd.
Lennox International, Inc.
LG Electronics, Inc.
Modine Manufacturing Co.
Parker Hannifin Corporation
Peerless of America, Inc.
Samsung Electronics Co., Ltd.
Tecumseh Products Company
The Trane Company
Valeo, Inc.
Visteon Automotive Systems
Wolverine Tube, Inc.
York International, Inc.

For additional information:

Air Conditioning & Refrigeration Center
Mechanical & Industrial Engineering Dept.
University of Illinois
1206 West Green Street
Urbana, IL 61801

217 333 3115

Refrigerant-Side Tradeoffs in Microchannel Evaporators

Abstract

The present study examined design issues of microchannel evaporators associated with the flow maldistribution caused due to header pressure gradient. The effects of mass flow maldistribution on microchannel heat exchanger were quantified by using a single port simulation model.

Longitudinal headers as currently used with microchannel condensers may not be suitable for the applications with microchannel evaporators. Mass flow maldistribution was investigated by using well-known pressure drop and heat transfer correlations for two-phase flow, selected after comparing with the results obtained by using different correlations. It was found that mass flow maldistribution cannot be controlled by changing either port/header diameter or the refrigerant state at the inlet to the port, but only by minimizing pressure gradients along header. At the same time the need to avoid phase separation in the header places a lower bound on mass flux.

The dependence of heat exchanger capacity on the diameter and the length of the longitudinal and radial headers and was investigated in detail. Results demonstrated that the requirement for inertially dominated flow in the inlet header severely limits the set of feasible evaporator geometries. Accordingly, alternative concepts for header design were suggested.

Introduction

Compact cross-flow heat exchangers with flat multi-port microchannel tubes and folded louvered fins have almost completely replaced conventional round tube flat fin condensers in automotive air-conditioning applications. Nearly all have two vertical headers partitioned to accommodate 3-5 passes consisting of multiple parallel tubes. Since void fractions exceed 90% in most of the headers, achieving near-uniform vapor distribution among hundreds of parallel refrigerant parts has not presented serious problems for condensers. However in evaporators the challenge is to distribute the liquid evenly among the microchannel ports. Because of the high liquid/vapor density ratio of fluorocarbon refrigerants, void fractions are generally ~ 90% at the evaporator inlet and exceed 90% at intermediate headers in higher-quality regimes.

Experimental data on microchannel evaporators are limited. Stott and Bullard [1] conducted experiments with microchannel evaporator (with port diameters ~ 0.7 mm), fed at four locations along the horizontal inlet header. They quantified maldistribution by measuring superheat on individual microchannel tubes, observing that some had nearly zero approach temperature differences while other exits were saturated, despite the TXV holding the aggregate suction superheat at 5°C. The tubes showing highest exit superheat were the ones that received most of vapor at their inlets. The experiments repeated for different refrigerant flow rates showed the same trend. In all the experiments, inlet header mass flux was less than 20% of the needed to maintain inertially-dominated fully-developed flow. Little is known about the flow regimes in developing two-phase flow, but it seems likely that the refrigerant would be highly susceptible to stratification at mass velocities significantly less than the 265 kg/m^2-s required for annular flow at these conditions [2].

Cho et al. [3] investigated flow maldistribution and phase separation in a microchannel evaporator with 15 tubes and aluminum header pipe with outer diameter of 22 mm at the mass flux of 60 kg/m^2-s. Mass flow rates were determined in each microchannel tube, along with the ratio of the quality in each microchannel tube to inlet quality

at the header. Severe mass flux and quality maldistribution was observed because of the extremely low refrigerant mass velocities in the header.

These experimental results suggest strongly that longitudinal headers such as those currently used with microchannel condensers may be unsuitable for applications with microchannel evaporators. Additionally, it may be necessary to maintain a certain minimum mass velocity in these headers to reduce maldistribution.

This paper identifies and examines important design issues associated with achieving uniform distribution in microchannel evaporators. Until this problem is solved, the technology will be limited, as it is now, to condensers of air conditioning systems. Since heat pumps must accommodate refrigerant flow reversals, this analysis is focused on single pass heat exchangers to eliminate the additional maldistribution risks associated with intermediate headers. The authors identified two causes of maldistribution: Header ΔP induced maldistribution and maldistribution of evaporator inlet quality. Interestingly, there is an upper bound on the performance degradation in evaporators due to maldistribution of quality; a brief discussion on quantification of performance degradation and ways to offset it could be found in Kulkarni and Bullard [4]. In this paper, the attention will be limited only to maldistribution caused due to header pressure gradient.

The next section reviews the current state of knowledge of two-phase pressure drop, heat transfer and void fractions in the sub-millimeter channels and headers of microchannel heat exchangers. Combining this information with a few simplifying analytical assumptions then leads to the identification of design constraints, which in turn are applied to three families of possible header designs. The results lead to the conclusion that longitudinal headers of the type heretofore used in microchannel condensers are least suitable for use in evaporators. The paper concludes with analyses of a proposed radial design, which appears to offer substantial advantages from the standpoint of refrigerant distribution.

Background

The superior air and refrigerant-side performance of microchannel heat exchangers has been documented extensively in the literature (Jacobi [5] and Garimella [6]). However there have been relatively few detailed investigations of two-phase heat transfer, pressure drop, flow regimes and void fractions in sub-millimeter ports. Therefore, the empirical database is still too sparse to support development of broadly-applicable correlations. Far less is known about the developing two-phase flow in the headers of microchannel heat exchangers, where diameters range from 10-30 mm. Most experience is with condensers where void fractions are high and maldistribution concerns are less important, so only a few detailed studies have been done. Zietlow [7] conducted flow visualization experiments and detailed measurements of refrigerant mass in microchannel condensers and concluded that a homogeneous void fraction assumption was valid across a range of typical operating conditions.

Most of the two-phase pressure-drop correlations currently available for refrigerants are based on experiments in tubes larger than 7, 4 and 3 mm (Souza and Pimenta [8], Friedel [9] and Zhang and Kwon [10] respectively). When extrapolated to diameters of 0.5 mm, they yield the results shown in Figure 1a for the range of mass fluxes considered in the current analyses. Figure 1a is based on the design operating conditions (T_{evap} = 12°C, D = 0.5 mm) and compared at x = 0.5. The choice of Zhang and Kwon [10] correlation for the purpose of this paper

was based on the excellent agreement observed between this correlation and experimental microchannel data of Nino [11].

Similarly Figure 1b shows some of the two-phase heat transfer correlations plotted in nondimensionalized form for operating conditions: T_{evap} = 12°C, G = 285 kg/m^2-s, D = 0.5 mm. Three correlations for two-phase evaporative heat transfer were considered. The first, Lazarek and Black [12], was based on R113 data in 3 mm tubes. Another by Liu and Winterton [13] was based on R12, R113, R11, R114 data in 2.95 mm tubes, while a third, Wattelet, et al [14] was developed from R12, R22, R134a and R410A data in tubes of diameter 7-11 mm. At design mass flux in this study, G = 285 kg/m^2-s, the source data for all three correlations lay in the annular flow regime, giving some degree of confidence that they may be applicable to other wetted-wall regimes such as the intermittent flows observed in microchannels (Coleman [15]). At 5.8 kW/m^2 design heat flux in the present study is in the range of the last two correlations, but less than the lower bound (14 kW/m^2) investigated by Lazarek and Black [12].

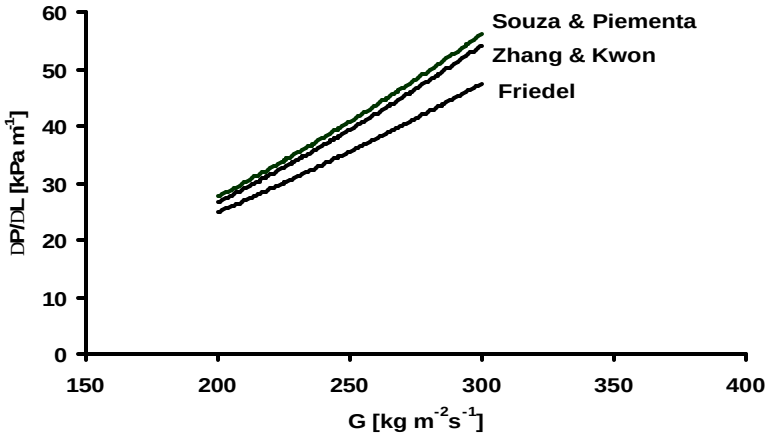

Figure 1 (a). Choice of 2-phase frictional pressure drop and heat transfer correlation (R410A D=0.5 mm Tevap = 12°C)

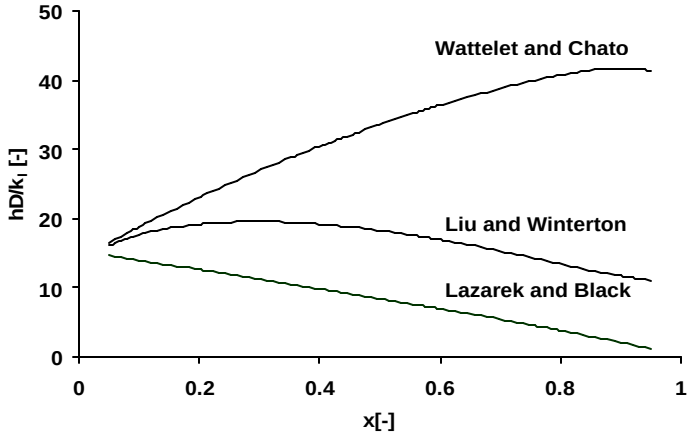

Figure 1 (b). Choice of 2-phase frictional pressure drop and heat transfer correlation (R410A D=0.5 mm Tevap = 12°C)

The Wattelet et al. [14] correlation was selected because it is the only one of the three based on R410A data. It also includes an explicit nucleate boiling term, whose contribution to the net heat transfer coefficient is greatest at higher reduced pressures that exist in R410A evaporators.

For single-phase heat transfer, the Gnielinski [16] correlation has been shown by Heun and Dunn [17] to give good agreement with data obtained in careful single-tube experiments. The single-phase pressure drop was computed using Churchill [18] friction factor.

Achieving uniform distribution

In conventional evaporators, uniform distribution of two-phase flow is achieved using a variety of proven methods, where the number of parallel circuits is generally less than 10. In microchannel heat exchangers, hundreds of parallel ports are generally fed from a cylindrical header as shown schematically in Figure 2. Even for the case of single-phase inlets (e.g. condensers, radiators), some mass flow maldistribution will occur because of inherent asymmetries in turning and inlet/exit losses, ac/deceleration and/or differing flow lengths (Yin et al. [19]). In condensers, the driving pressure differential along the parallel circuits is also influenced by the density and velocity differences in the vapor inlet/liquid outlet headers. Of course for evaporators the situation is further complicated by the fact that inlet density is very sensitive to operating condition (condenser outlet enthalpy). Finally, the absence of correlations describing developing two-phase flow makes it necessary to make crude simplifying assumptions to describe the pressure gradient and void fraction in evaporator inlet headers.

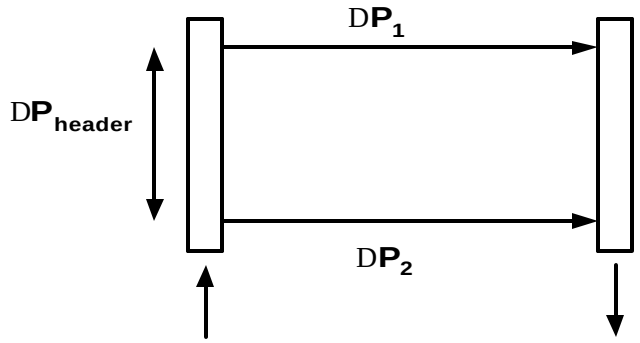

Figure 2. Effect of header pressure gradient

Fortunately as the following parametric analyses will illustrate, the differences among several families of header geometries are not very sensitive to these simplifying assumptions. Therefore future investigations can be redirected away from existing header designs and focused on other concepts that appear more promising. Ideally the refrigerant flow in the inlet header, where quality ~ O(10-25%) would be misty and homogeneous, a regime not observed below G ~2000 kg/m^2-s (for standard operating conditions and D_{header} = 9 mm, T_{evap} = 12°C, x_{evap} = 20%, etc) for fully-developed refrigerant flow in this quality range (Thome et al. [2]). Such very high mass fluxes, if present, could create large pressure gradients along the headers, exacerbating maldistribution among the parallel circuits. Therefore the following para metric analyses focus on a range of mass fluxes lying just above a minimum level where the effects of gravity diminish and the flow becomes inertially dominated (i.e., beyond the wavy-stratified regime). Although these flow regime boundaries are imprecise – even for developed flows – and strictly

inapplicable to developing flows, they are helpful in focusing the analyses on inertially-dominated flows that are more likely to - expose all microchannel ports to nearly the same time-averaged inlet quality.

Header DP-induced mass flux maldistribution

Pressure gradients in the header can result in each parallel circuit seeing a different driving pressure differential. Figure 2 shows a schematic of microchannel heat exchanger where the refrigerant enters from the bottom. As it flows through the header, pressure drops due to friction and rises due to deceleration as part of the refrigerant exits the header to flow through the microchannel ports. In general the driving pressure seen by different tubes is different, so each tube receives a slightly different refrigerant mass flow rate at its inlet.

To explore the effect of mass flow maldistribution on heat exchanger capacity, a single port simulation model was developed. The single-port microchannel is divided into many finite elements along its length, and the two-phase or superheated heat transfer and pressure drops are computed within each. For this analysis, the air-side heat transfer coefficient was assumed constant at 90 W/m^2-K and the ratio of air-side area to refrigerant-side area (A_{ratio}) was assumed to be 4. Evaporating temperature (T_{evap}) was considered to be 12°C and inlet quality (x_{in}) 24%, corresponding to isenthalpic expansion of R410A from a condenser exit at 45°C saturation temperature and 5°C subcooling. Tube length was selected such that the total in-tube pressure drop (expressed as drop in saturation temperature ΔT_{sat}) is 2°C and that a TXV controls refrigerant exit superheat at 5°C. These assumptions yield a tube-length 1.1 m and a refrigerant flow rate of 285 kg/m^2-s of refrigerant and approximately 9 W heat transfer per port.

The assumption of ΔT_{sat} = 2°C warrants some explanation. Parallel circuiting could theoretically eliminate refrigerant pressure drop, but that would exacerbate the effect of header pressure gradients on the driving pressure differential seen by the tubes, as observed in a prototype system by Stott and Bullard [1]. Some "plenum effect" is necessary, but larger pressure drops reduce compressor efficiency so it is assumed here that microchannel evaporators will be designed for approximately the same pressure drop as conventional ones.

Figure 3 shows the effect of header pressure gradient, which reduces total heat transfer in tubes receiving lower refrigerant mass flux (due to maldistribution). Thus, for R410A (D=0.5 mm) when the "average" tube sees a pressure differential of ΔT_{sat} = 2°C, a tube experiencing ΔT_{sat} = 1°C, will have ~20% lower heat transfer, due to the effect of lower mass flux. Another tube seeing ΔT_{sat} = 3°C will have only slightly greater heat transfer, because the increase is limited as the short superheated segment is replaced by a slightly colder two-phase region. Downstream, the exits from the two tubes must combine to produce 5°C superheat: a very highly superheated (low flow) stream mixing with a two-phase one having slightly increased mass flow. An expansion device adjusted to maintain 5°C superheat would therefore react to such maldistribution by delivering a total mass flow lower than the case where flow is evenly distributed among the tubes. It is apparent from Figure 3 that it would be desirable to limit header pressure gradients to approximately 0.2°C to ensure that degradation of total heat exchanger capacity is limited to about 4-5%.

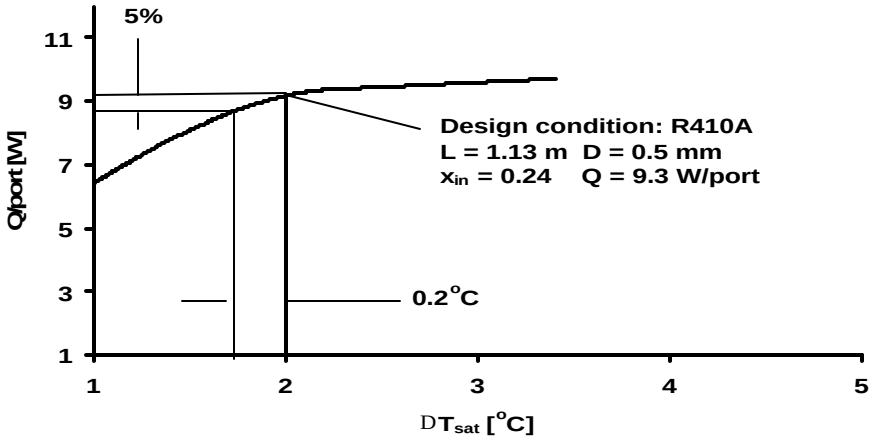

Figure 3. Effect of header ΔP induced mass flux maldistribution on heat exchanger capacity

It is best to minimize the header pressure gradient-induced mass flux maldistribution by selecting geometries that make mass flux as insensitive as possible to the driving pressure differential. Thus it is essential to minimize $dG/d(\Delta T_{sat})$ which in general a function of channel diameter, refrigerant inlet quality and thermophysical properties of the refrigerant.

Figure 4 shows how mass flux can be affected by variations in driving pressure differential, for the tube length shown. These "design" tube lengths were determined for different diameters similarly (imposing $\Delta T_{sat} = 2°C$ and $dT_{sup} = 5°C$). Since the lines of D = constant are close to one another, it is apparent that small (i.e. <5%) manufacturing-related variations among port diameters are unlikely to cause significant mass flow maldistribution. The nearly identical slopes $dG/d(\Delta T_{sat})$ make it clear that the mass flow sensitivity can not be minimized by changing D, so maldistribution must be addressed by minimizing pressure gradients along headers.

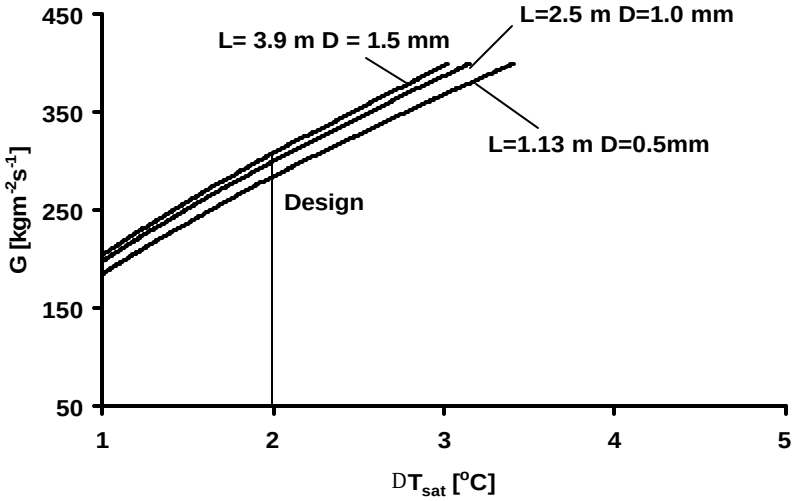

Figure 4. Effect of D_{port} on $dG/d(\Delta T_{sat})$

Additional simulations were conducted to explore the effect of system operating conditions that influence the evaporator. It was found out that the slope of the G vs ΔT_{sat} curve remained independent of inlet refrigerant qualities. This implies that the effects of header ΔP induced maldistribution will be unaffected by variations of condenser exit enthalpy resulting from changes in outdoor air temperature. The slope of G vs ΔT_{sat} curve *is* a function of refrigerant properties as simulations conducted with R22 and R134a revealed. It was noticed that the low pressure refrigerants required shorter tubes (0.78 and 0.58 m for R22 and R134a respectively). The curve was flatter for R134a, indicating less susceptibility to maldistribution.

From the above single port analyses, it is possible to infer several guidelines for microchannel evaporator designs. First note that the refrigerant state at the evaporator inlet is fixed by condenser exit conditions and the evaporating pressure. The port diameter is selected in the usual manner as a result of tradeoffs among the desired pressure drop, heat transfer per circuit, number of circuits and refrigerant charge. Once the port diameter and the refrigerant condition at the inlet to the evaporator are fixed, the single tube simulation model computes the length of the circuit (single port) and the required refrigerant mass flux through it. Again, the example results shown in Figure 3 are based on limiting the drop in saturation temperature at 2°C and requiring that the refrigerant exits in a superheated state (superheat = 5°C, so that liquid refrigerant droplets do not enter the compressor).

At this point the header design is not decided. Figure 3 showed that header pressure gradients causing 10% variations among single-port pressure differentials will cause some ports to get higher refrigerant mass flow while others get lower, resulting in a 4-5% lower heat transfer rate for R410A microchannel (D=0.5 mm) evaporator. Thus, mass flux maldistribution (caused by pressure gradient in the header) cannot be controlled by changing either the port diameter or the refrigerant state at the inlet to the port. Therefore, the issue of mass flux maldistribution must be addressed through header design.

Header design tradeoffs

Constraints on header design are now becoming clear. Header diameter must be sufficient to carry the refrigerant flow required for the specified evaporator capacity. Header mass flux must be high enough to avoid gravitationally-induced liquid-vapor stratification, yet low enough to maintain near-uniform driving pressure gradients seen by the parallel ports. Header pressure gradients are affected by both friction and deceleration, as refrigerant leaves the header and enters the tubes. Nevertheless, in the terminal portion of the header the refrigerant velocity approaches zero, where stratification cannot be avoided without radically varying header cross-sectional area. Therefore it is necessary to impose several design constraints, rather arbitrarily, in order to identify the feasible design space in which more detailed analyses can be conducted. The first constraint is to limit the header-induced saturation temperature (pressure) gradient to lower than 0.2°C, to place an upper bound on ΔP-induced maldistribution. The second is to limit the potential for gravitational stratification to a small segment near the end of the header by specifying that header mass flux exceed a lower limit G_{min} throughout the rest of the header. Empirically developed flow regime maps developed by Thome et al. [2] are strictly applicable only for horizontal fully developed flow, but they suggest that stratified flow of R410A at typical inlet header qualities ~20-25% can be avoided for G>200 kg/m^2-s. For the same reasons it was necessary to use a frictional pressure drop correlation that

applies only to fully developed flow; one that was based on R410A data and tube diameters in the 7-10 mm range [8] was selected.

Despite the approximate and somewhat arbitrary nature of these constraints, the following analyses will show that they are sufficient to eliminate some potential header designs, and to suggest some rather novel designs that might be necessary to minimize refrigerant maldistribution in microchannel evaporators.

Longitudinal header

A schematic of a longitudinal header is shown in Figure 5. By making a few simple geometric assumptions applicable to most heat exchangers, of this type, it is possible to derive equations that identify a subset of designs most likely to provide well-distributed refrigerant flows.

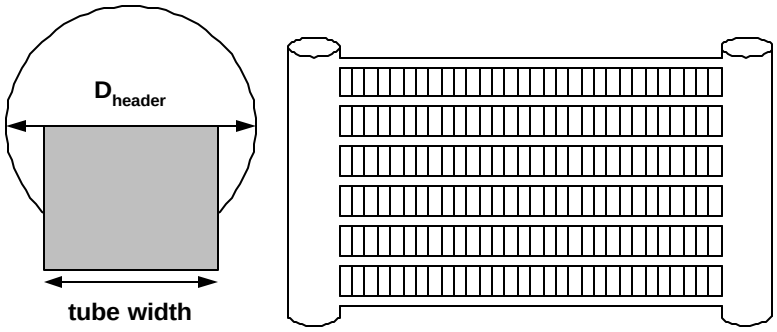

(a) (b)

Figure 5. Longitudinal header ((a) cross-section and (b) as used in a full heat exchanger)

The header diameter is defined by the number of ports, the protrusion of tubes almost to the header centerline reduces the effective (hydraulic) diameter of the header as shown in Figure 5a. Recall that heat transfer capacity per port was determined by the port diameter, so the total number of ports will be determined by the desired heat exchanger capacity. However, the number of ports per tube cannot be selected arbitrarily, because it is related to header diameter by the approximate relationship

$$D_{header} = 1.5*N_p*D_p \quad (1)$$

where the factor 1.5 allows for web and wall thicknesses plus some clearance within the header as shown in Figure 5a. In microchannel heat exchangers used by Kirkwood and Bullard [20], tube width is typically 1.4 times the number of ports times port diameter.

Also the header length is determined indirectly by the port diameter

$$L_h = N_t*(F_h + D_p + 2*t_{wall}) \quad (2)$$

where the fin height (~1 cm) and tube wall thickness (~0.2 mm) are determined for all heat exchangers by fin efficiency and burst pressure considerations, respectively.

If it is required for the inlet header to have inertially dominated flow over a fraction f of its length then refrigerant mass flux will decrease linearly from its maximum at the header inlet to the value G_{min} at length fraction f.

$$G_{min} = (1-f)*N_p*N_t*G_p*D_p^2/D_h^2 \quad (3)$$

The critical mass flux for the baseline R410A operating conditions cited earlier, G_{min} ~ 172 kg/m^2-s (to get 10 kW and have 90% of longitudinal header to have inertially dominated flow) defines the lower bound on the mass flux in the header for which the refrigerant flow in the header is inertially dominated.

Calculations of header pressure drop and the resulting mass flows proceed tube-by-tube down the header, conservatively assuming uniform pressure in the exit header to obtain an upper bound on refrigerant mass flow distribution. Figure 6 shows the combined effect of these constraints. To ensure that the 2-phase flow is inertially dominated in at least 90% of the header, longitudinal headers less than 1 m long must have diameter less than 10-12 mm, so the microchannel tubes must be of approximately of the same width. Figure 7 shows that such an evaporator with a 1-m inlet header would have a capacity of about 45 kW! The same graphs imply that a smaller (say 10 kW) evaporator would need an inlet header about 0.45 m long and an air flow depth (tube width) of only ~6 mm. Heat transfer capacity achievable from the refrigerant fed through this header is shown in Figure 7. It rises rapidly because the total heat transfer area increases with the number of ports/tube and number of tubes. The pressure gradient in the header (drop due to friction and rise due to deceleration) is shown in Figure 8, increasing with header length because of the higher inlet mass flux needed to feed the larger number of tubes. It is seen that attempts to limit the stratified section to less than 10% of header length could cause header pressure gradient to exceed 0.2°C, which could exacerbate maldistribution by creating larger pressure differentials among the heat exchanger tubes. The limitations of longitudinal headers are now clear. For residential-scale applications (<10 kW) the headers could be of reasonable length (<0.45 m) but so thin (<6 mm) that extremely large face areas would be required. The same kind of packaging problem would exist for a 100 kW (~ 30 ton) commercial-scale rooftop unit.

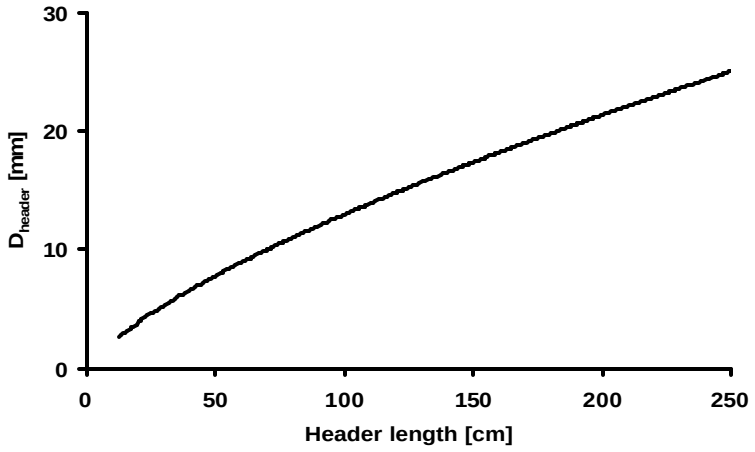

Figure 6. Geometry of a 90% inertially dominated longitudinal header

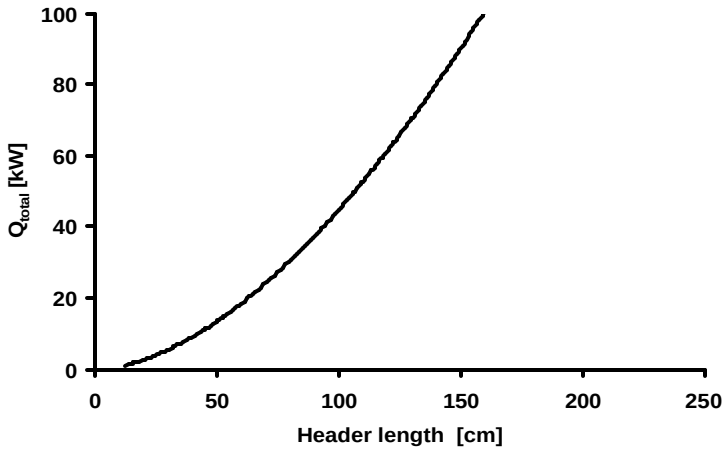

Figure 7. Capacity of a 90% inertially dominated longitudinal header

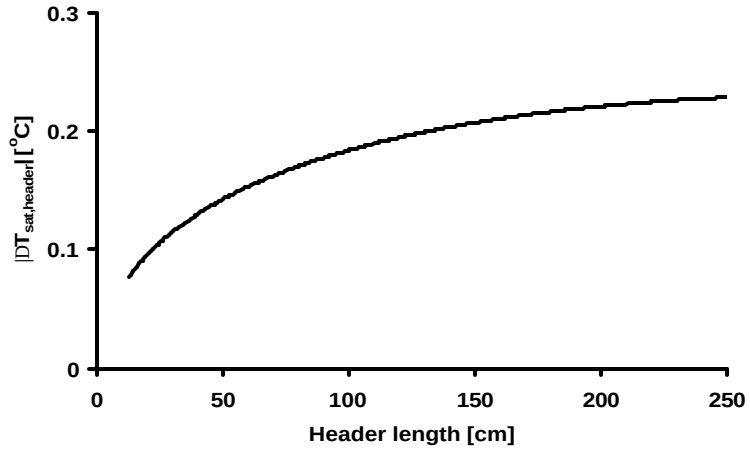

Figure 8. Header ΔP (ΔT_{sat}) for a 90% inertially dominated longitudinal header

Radial header

Consider a new kind of radial header design, as shown in Figure 9 with multiport tubes located along its circumference. It can be shorter than longitudinal headers because the port density is not limited by the tube width, so it can handle a larger refrigerant mass flow rate with less frictional pressure drop. Fortunately, extruded aluminum microchannel tubes can be easily bent for routing to the evaporator core, and symmetrically located to ensure that all tube lengths are identical.

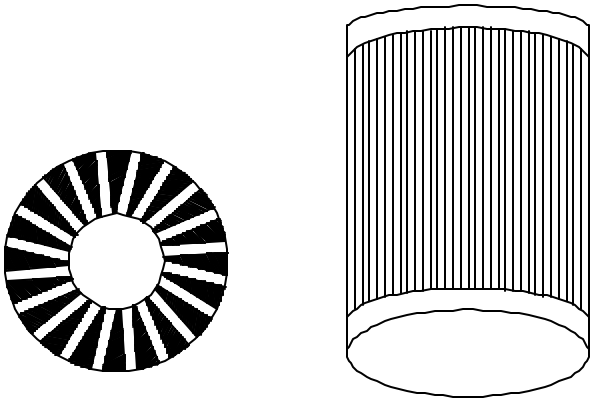

Figure 9. Radial header (cross-section and viewed from top)

The governing equations for a radial header are very similar to those for the longitudinal header; only the geometric constraints differ:

$$L_h = 1.5*N_p*D_p \quad \text{and} \quad N_t \leq \pi* D_h/(D_p+2*t_{wall}) \qquad (4)$$

Besides accommodating more tubes per unit length, the tube width (#ports/tube) can now be increased to make the heat exchanger deeper and face area smaller to meet packaging constraints.

The results are shown in Figures 10-12 for the case of equality in equation for the number of tubes, and suggest clear performance advantages of the radial header design over the longitudinal header design. The radial header is shorter, so it is easy to avoid stratification over 90% of its length while at the same time achieving a lower header pressure gradient. In fact the pressure gradient is quite small, because friction is almost completely offset by deceleration. If manufacturing constraints do not allow tubes to touch along the interior circumference, capacity would be reduced accordingly. Since the number of tubes is lower, the refrigerant mass flux in the header, capacity per unit length and pressure gradient are lower. Thus longer radial headers would be required to achieve the same evaporator capacity.

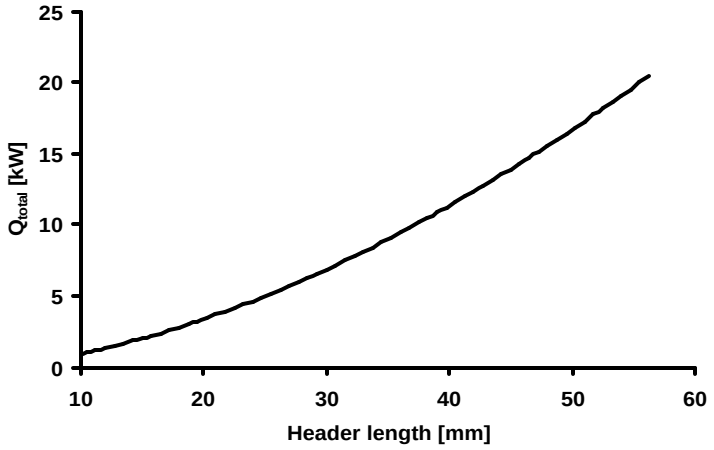

Figure 10. Capacity of a 90% inertially dominated radial header

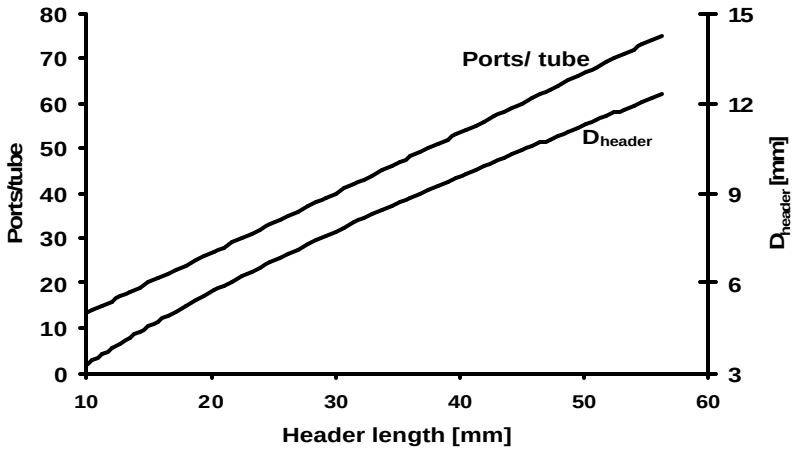

Figure 11. Geometry of a 90% inertially dominated radial header

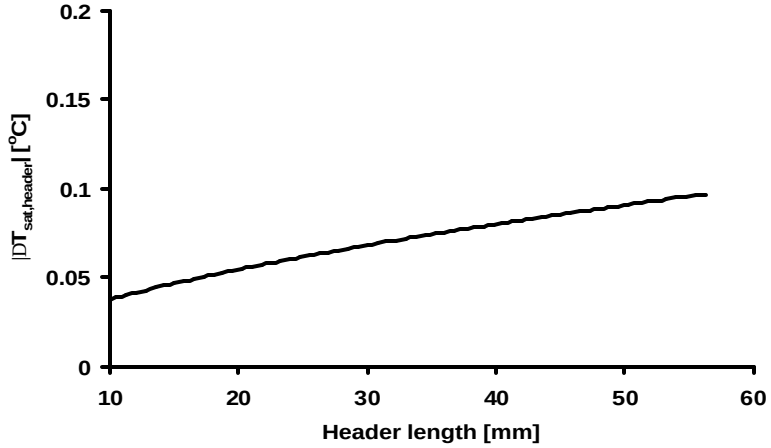

Figure 12. Header ΔP (ΔT_{sat}) in a 90% inertially dominated radial header

Effects of simplifying assumptions

"Minor" pressure drops in tubes

Having established the general outlines of feasible heat exchanger geometries for evaporators employing longitudinal or radial headers, it is necessary to quantify the magnitudes of other effects that were neglected.

Since prototype microchannel evaporators are being designed with vertical tubes to facilitate condensate drainage, it is necessary to consider gravitational effects in a vertical tube. If the tube of length = 1.13 m is designed to be vertical and refrigerant flow is vertically downwards, there is pressure gain due to gravity and pressure loss due to friction. If the flow is vertically upwards, pressure drop is the sum total of drop due to friction and gravity. In the former case, the compressor work is slightly lower because of pressure gain due to friction and in the latter case the compressor work is slightly higher. The pressure drop (or gain) due to gravity in a vertical tube of length =1.13 m is 12 kPa (about 18% of the pressure drop due to friction). Usually a microchannel tube will be serpentined several times to reduce the height of the heat exchanger. In that case the gains due to reduced pressure drop (in the

former case) and losses due increased pressure drop (in the latter case) will be reduced. The upper bound on the pressure drop due to gravity is ~ $\rho_{fg}*g*L_{tube}/N_{serpentine}$

The pressure drop due to acceleration is about 2 kPa, about 3% of the pressure drop due to friction.

The foregoing analysis also neglected other pressure drop terms in tubes, due to the sudden contraction experienced by refrigerant when entering from the header (D ~ 15-20 mm) space into the ports (D < 1 mm), and the sudden expansion when exiting from the port to the outlet header. The change in static pressure at a sudden contraction is the sum of frictional dissipation and theoretical kinetic energy change. According to Collier and Thome [21], this change for a homogeneous flow is given by:

$$?P_{contraction} = 1/2 * G_p^2 * v_f * \left[(1/C_c - 1)^2 + \left(1 - (A_p/A_h)^2\right)\right] * \left[1 + \left(\frac{v_{fg}}{v_f}\right) * x\right] \qquad (5)$$

at the design conditions for header sizes of the order of 10-15 mm, area ratio ($A_p/A_h \rightarrow 0$ effectively) where ($1/C_c$ – 1) was found to be 0.5. (Collier and Thome, 1994). Each port is assumed to receive the same refrigerant quality at its inlet (x=0.24). The value of $\Delta P_{contraction}$ under these conditions was found to be 0.3 kPa (0.0092°C) or about 0.5% of $\Delta P_{friction}$ for a single isolated microchannel port. However, recent measurements by Nino, et al (2001) exceeded this estimate by factors of 3-4, and the difference was attributed to the webs between the microchannel tubes. However, the results were typical for the geometry used by Nino et al [11]; hence, due to lack of generalized correlations, equation (5) was used in the present work.

The irreversible pressure drop due to sudden expansion of 5°C superheated refrigerant exiting the port into the header was also found to be small (~1.4% of $\Delta P_{friction}$). It was estimated using the method of Idelchik [22] by (for Reynolds number based on port diameter>3500)

$$?P_{expansion} = G_p^2/(2*?_v) \qquad (6)$$

Note that this expression is for pressure loss at the sudden expansion and neglects the effect of velocity change during the expansion process. Detailed experiments with single phase nitrogen in a microchannel heat exchanger by Yin et al. [19] demonstrated that the available pressure drop correlations, such as those cited above, could produce satisfactory estimates of these “minor pressure losses”.

Header pressure drop due to gravity

Next, consider pressure drop in a vertical header due to gravity. Consider a header with height L_h oriented with the horizontal at an angle θ. If the refrigerant enters from the bottom of the header, the pressure drop due to gravity is given by:

$$?P_{gravity} = g * L_h * \sin(q) * ((1-a)*?_l + a*?_v) \qquad (7)$$

Where α is Zivi’s void fraction. The effect of pressure drop due to gravity is to increase the header pressure drop. Again if the header is vertical and the refrigerant flow is from the bottom, the pressure drop due to friction and pressure due to gravity add up and the net pressure gain due to deceleration is lowered. If the refrigerant flows from top to the bottom in the header, pressure gain due to gravity adds up to pressure gain due to deceleration. The pressure drop (gain) is usually about 0.1°C/m, which again points to the need of short headers.

Sensitivity of results to different correlations

Due to lack of data, there are no universally accepted two-phase heat transfer and pressure drop correlations for evaporation in microchannel tubes. The results presented here, however, are relatively insensitive to the choices made. For example, the Liu & Winterton [13] or Lazarek & Black [12] two-phase heat transfer correlations would have increased the design tube length only 3.5% and 20%, respectively, requiring corresponding reductions in capacity and increases in the number of tubes required. The results are less sensitive to the choice of the pressure drop correlations as shown in Table 1. Using Souza & Piementa [8] would decrease design tube length by only 2%, while Friedel [9] correlation would increase it about 11%.

Table 1. Sensitivity of results to different correlations (two-phase frictional ΔP)

Correlation used	L [m]	Q [W]	G [kg $m^{-2}s^{-1}$]
Zhang & Kwon [10]	1.13	9.3	285
Souza & Piementa [8]	1.11	9.0	279
Friedel [9]	1.25	10.3	320

Further, in case of two-phase heat transfer coefficients, the need for accuracy is less, because the relatively large refrigerant-side area reduces refrigerant-side resistance so dramatically in flat multiport tubes, yielding air/refrigerant area ratios of about 4:1, compared to the 20:1 ratio typical of round tube flat-fin heat exchangers. Single-tube condensation studies suggest that macrochannel correlations can be extrapolated to microchannels without substantial loss of accuracy (Garimella [6]). However there are even fewer studies available on microchannel evaporators, mainly because of concerns about refrigerant maldistribution. The results in Table 2 successfully demonstrate that the choice of two-phase heat transfer correlation does not affect the results significantly.

Table 2. Sensitivity of results to different correlations (two-phase h_{ref})

Correlation used	L [m]	Q [W]	G [kg $m^{-2}s^{-1}$]
Wattelet et al. [14]	1.13	9.3	285
Lazarek & Black [12]	1.35	8.4	260
Liu & Winterton [13]	1.17	8.9	278

None of the foregoing simplifying assumptions, therefore, would have a significant effect on the main conclusion: namely longitudinal headers (as currently designed for condensers) pose severe risks of refrigerant maldistribution when the cycle is reversed for heating mode. New designs such as the radial configuration suggested here, warrant experimental investigation.

Conclusions

The effects of mass flow maldistribution on microchannel evaporator was investigated by using a single port simulation model. Header pressure gradient was limited approximately 0.2°C to keep the degradation of total heat exchanger capacity below ~5%.

The mass flow maldistribution was estimated by using well-known pressure drop and heat transfer correlations for two-phase flow after comparing with the results obtained by using different correlations. It was found that mass flow maldistribution cannot be controlled by changing either port/header diameter or the refrigerant

state at the inlet to the port, but only by limiting pressure gradients along header. This limitation, combined with a requirement that the flow be inertially-dominated in order to prevent quality-induced maldistribution, suggests that microchannel evaporators equipped with conventional longitudinal headers must be extremely thin and therefore have very large face areas to achieve a given design capacity. An innovative radial header design was proposed and subjected to similar analyses, and the results suggest that distribution could be minimized in evaporators having exterior package dimensions typical of those in use today.

The results of this analytical investigation offer hypotheses to be tested using the next generation of microchannel heat exchanger designs.

References

[1] Stott SL, Bullard CW, Dunn WE. Experimental Analysis of a Minimum-TEWI Air Conditioner Prototype. University of Illinois at Urbana-Champaign 1999, ACRC CR-21.

[2] Thome JR, Kattan N, Favrat D. Flow boiling in horizontal tubes: Part1- Development of a diabatic two-phase flow pattern map. Trans of ASME Journal of Heat Transfer 1998; 120:140-47

[3] Cho H, Cho K, Youn B, Kim Y. Flow maldistribution in microchannel evaporator. submitted to 9th International Refrigeration and Air-Conditioning Conference at Purdue, 2002.

[4] Kulkarni T, Bullard CW. Optimizing Effectiveness of R744 Microchannel Evaporators. submitted to 5th IIR-Gutsav Lorentzen Conference on Natural working fluids, 2002.

[5] Jacobi AM. High Performance Heat Exchangers for Air Conditioning and Refrigeration Applications (Non-circular tubes). ARTI 21-CR Project 20020-Phase 2, 2001.

[6] Garimella S. Microchannel Gas Coolers for Carbon Dioxide Air-conditioning Systems. ASHRAE Transactions 2002;108(1) (in press)

[7] Zietlow DC, Pedersen CO. Flow Regime Mapping and Analysis of R-134a in a Small-Channel Cross-Flow Condenser. ASHRAE Transactions 1998; 104(2): 540-47

[8] Souza AL, Pimenta MM. Prediction of pressure drop during horizontal two-phase flow of pure and mixed refrigerants. ASME conf. Cavitation and Multiphase Flow 1995;21:161-71

[9] Friedel L. Improved friction pressure drop correlation for horizontal and vertical two-phase pipe flows. Presented at European two-phase flow group meeting, Ispra, Italy, paper t2, 1979.

[10] Zhang M, Kwon SL. Two-phase frictional pressure drop for refrigerants in small diameter tubes. Proceedings of the International Conference on compact Heat Exchangers and Enhancement Technology for the process Industries, 1999 July; Banff, Canada, p.285-92

[11] Nino V, Payne W, Hrnjak PS, Newell TA, Infante Ferreira CA. Two-phase pressure drop in microchannels. IIF-IIR- Commission B1-Paderborn, Germany, 2001 (submitted for publication).

[12] Lazarek G M, Black SH. Evaporative Heat Transfer, Pressure Drop and Critical Heat Flux in a Small Vertical Tube with R-113. Int. J. Heat Mass Transfer 1982; 25(7):945-60.

[13] Liu Z, Winterton RHS. Wet Wall Flow Boiling Correlation with Explicit Nuclear Term. Presented at the 5th Miami Int. Symp. On Multiphase Transport and Particulate Phenomena, 1988.

[14] Wattelet JP, Chato JC, Souza AL, Christoffersen BR. Evaporative Characteristics of R-12, R-134a, and MP-39 at Low Mass Fluxes. ASHRAE Transactions 1994;100(1):603-15.

[15] Coleman J, Flow Visualization and Pressure Drop for Refrigerant Phase Change and Air-water Flow in Small Hydraulic Diameter Geometries. Ph.D. Thesis, Mechanical Engineering, Iowa State University, 2000.

[16] Gnielinski V. New equations for Heat and Mass Transfer in Turbulent pipe and channel Flow. Int. Chem. Eng., 1976; 16:359-68.

[17] Heun MK, Dunn WE. Principles of Refrigerant Circuiting with Application to Microchannel Condensers: Part I - Problem Formulation and the Effects of Port Diameter and Port Shape. ASHRAE Transactions 1996; 102(2):373-81.

[18] Churchill SW. Comprehensive Correlating equations for Heat, Mass and Momentum Transfer in Fully Developed Flow in Smooth Tubes. Ind. Eng. Chem. Fundam. 1977;16 (1):109-16.

[19] Yin JM, Bullard CW, Hrnjak PS. Single phase pressure drop measurements in a Microchannel Heat Exchanger. Heat Transfer Engineering 2002; 23:1-10.

[20] Kirkwood AC, Bullard CW. Modeling, Design and Testing of a Microchannel Split-System Air Conditioner. University of Illinois at Urbana-Champaign 1999, ACRC TR-149.

[21] Collier JG, Thome JR. Convective Boiling and Condensation, 3rd Ed. Oxford: Oxford University Press, 1994.

[22] Idelchik IE, Handbook of Hydraulic Resistance, 3rd Ed. CRC Press, 1994.

Nomenclature

A = area [m^2],

dG = mass flux difference [$kgm^{-2}s^{-1}$],

dT = temperature difference [°C],

ΔP = pressure drop [kPa],

ΔT = drop in temperature [°C],

D = diameter [m],

F = fin,

g = acceleration due to gravity [ms^{-2}],

h = heat transfer coefficient [$W\ m^{-2}\ K^{-1}$]

G = mass flux [$kgm^{-2}s^{-1}$],

L = length [m],

N = number,

P= pressure [kPa],

Q = heat transfer capacity [W],

Re = Reynolds number,

t = thickness [m],

T = temperature [°C],

x = refrigerant quality [-]

Subscripts

evap = evaporating,

exp = expansion,

f = liquid,

g = gas,

h = header,

in = inlet,

l = liquid,

min = minimum,

p = port

ref = refrigerant

sat = saturation

t = tube

v = vapor

Greek letters

α = void fraction

θ = angle of inclination

ρ = density